ISSN 1063-7737, Astronomy Letters, 2016, Vol. 42, No. 12, pp. 783–789. © Pleiades Publishing, Inc., 2016.
Original Russian Text © I.S. Proshina, A.Yu. Kniazev, O.K. Sil'chenko, 2016, published in Pis'ma v Astronomicheskii Zhurnal, 2016, Vol. 42, No. 12, pp. 861–868.

# Counter-rotating Gas Disk in the S0 Galaxy IC 560

**I. S. Proshina[1*], A. Yu. Kniazev[1,2,3], and O. K. Sil'chenko[1**]**

[1] *Sternberg Astronomical Institute, Moscow State University, Universitetskii pr. 13, Moscow, 119992 Russia*
[2] *South African Astronomical Observatory, P.O. Box 9, Observatory, Cape Town 7935, South Africa*
[3] *Southern African Large Telescope (SALT), Cape Town, South Africa*

Received May 12, 2016

**Abstract**—A counter-rotating gas disk has been detected in the SA0 galaxy IC 560 located at the periphery of a sparse group of six late-type galaxies. The pattern of gas excitation and mid-infrared colors are indicative of ongoing star formation within 1 kpc of the center. Outside the gas disk with star formation the large-scale stellar disk of the galaxy has an old age and a very low metallicity, $[Z/H] \approx -1$. The source of external gas accretion onto IC 560 is undetected; the only option is a single infall of a companion rich in high-metallicity gas.

**DOI:** 10.1134/S1063773716120057

Keywords: *galactic kinematics, galactic disks, galactic evolution.*

## INTRODUCTION

Lenticular galaxies possess reddish stellar disks without any outstanding features and are believed to be "passive," i.e., forming no stars at the present epoch. However, on closer inspection, most of them turned out to contain appreciable amounts of cold gas (Welch and Sage 2003; Sage and Welch 2006). Why is there no noticeable star formation in S0 galaxies despite the presence of gas in them? The answer to this question may be the key to the entire evolution of disk galaxies that, as it becomes increasingly clear, is determined by the regime of external gas accretion onto the disk.

It is in lenticular galaxies that there is often a mismatch between the rotation of gas and the rotation of stars, implying that the currently observed gas is not the gas from which the disk stars were formed sometime in the past. At early stages of research on gas kinematics in S0 galaxies based on small samples randomly drawn from the populations of the field, groups, and clusters, it was estimated that about a quarter of all gas disks in S0 galaxies rotate in the opposite direction to the stellar disks (Kuijken et al. 1996): this was found from long-slit spectroscopy, when the slit was placed along the major axis of the isophotes (the probable line of nodes) of galactic disks, i.e., the authors dealt with the rotation velocity projected on the line of nodes of the stellar disk. Kuijken et al. (1996) also noted that the fraction of S0 galaxies with a counter-rotating *stellar* component in the disk is much lower, no greater than one percent. This is consistent with the apparent absence of current star formation in the gas disks of most S0 galaxies. Subsequently, when the studies of complete (in volume) samples (Cappellari et al. 2011) of early-type galaxies, with S0 galaxies again constituting most of them, appeared (these studies were carried out by the methods of panoramic spectroscopy, allowing the direction of the rotation axis to be determined accurately), the fraction of galaxies with mismatched rotation of gas and stars was found to depend strongly on the density of the environment: there are a factor of 4 more of them in the field than in the Virgo cluster (Davis et al. 2011). We then studied a sample of absolutely isolated S0 galaxies, i.e., objects in an extremely rarefied environment, and exactly half of the gas disks among absolutely isolated S0 galaxies turned out to exhibit apparent counter-rotation with respect to the stars in projection on the line of nodes of the stellar disks (Katkov et al. 2015); this means that in the idealized situation of the arrival of external gas from an arbitrary direction all gas disks in isolated S0 galaxies were acquired through recent accretion. There is seemingly some paradox here: if a galaxy is absolutely isolated, then there is no visible accretion source near it. However, even isolated galaxies have small gas-rich companions, which can fall to the disk without disrupting it; at the same time, no individual reservoirs of *cold* gas can survive in a cluster, in the environment of hot

*E-mail: ii.pro@mail.ru
**E-mail: olga@sai.msu.su

X-ray gas, in the field of powerful gravitational tides from individual companions and from the cluster as a whole, and accretion is impossible in principle.

In this paper we present yet another new example of an S0 galaxy with a counter-rotating gas disk, this time not a strictly isolated one but belonging to a very sparse group of galaxies. This is the small lenticular galaxy IC 560 at a distance of 23 Mpc from us (NED), seen nearly edge-on, with the color indices $g-r=0.90$ and $u-r=2.72$ (SDSS), i.e., definitely belonging to the red sequence. It entered the ATLAS-3D sample almost exactly above the lower boundary of the luminosity range of the sample, $M_K=-22.1$ (Cappellari et al. 2011) and was classified as a "fast rotator" (Emsellem et al. 2011), which is absolutely typical of small lenticular galaxies. However, the gas component of this galaxy was not discussed within the framework of the ATLAS-3D survey, because neither neutral nor molecular hydrogen was detected in it. Nevertheless, there is an ionized gas at the center of this galaxy, it is noticeable and, as we suspected even when analyzing the data of the ATLAS-3D sample, counter-rotates with respect to the stars. To estimate the physical properties of the gas (and stars) and the extent of the gas disk in IC 560, we undertook new spectroscopic observations of this galaxy at the 11-m SALT telescope of the South African Astronomical Observatory with the long-slit RSS spectrograph.

## OBSERVATIONS AND DATA ANALYSIS

The galaxy IC 560 was observed with the long-slit RSS (Robert Stobie Spectrograph) spectrograph (Burgh et al. 2003; Kobulnicky et al. 2003) at the 11-m Southern African Large Telescope (SALT) on two nights in January 2013, with a total exposure time of 30 min on January 4, 2013, and 30 min on January 6, 2013. Thus, the total exposure time was 1 h. The spectrograph slit was positioned along the major axis of the galactic disk isophotes, $PA=15^\circ$; the slit width was $1.25''$. The PG0900 volume-phase grism provided a spectral resolution of 5.5 Å in the spectral range 3760–6860 Å "stitched" together from three pieces with small gaps between them (the RSS camera is a mosaic of three CCD detectors). The scale along the slit for readout with fourfold binning was $0.507''$ per pixel. The RSS effective field of view is 8 arcmin along the slit; therefore, at the small sizes of IC 560 the sky background to be subtracted from the object's spectrum was successfully measured at the edges of the slit of the galaxy's exposed spectrum. The comparison spectrum of an argon lamp was used for the wavelength calibration; our measurements of the positions of sky lines in the linearized spectrum shows that the resulting accuracy of the wavelength scale is 0.04 Å. The spectrophotometric standards were observed with the same spectroscopic RSS configuration at twilight and were used to correct the relative spectral flux. The spectra were initially assembled with the standard SALT reduction pipeline (Crawford et al. 2010), while the subsequent reduction was performed by the technique developed by Kniazev et al. (2008).

We used the spectra reduced in this way, with the subtracted sky background and corrected for the relative spectral sensitivity, to study the changes in the following spectral characteristics along the slit with distance from the galactic center: the line-of-sight velocities of the stars and ionized gas, the equivalent widths of the H$\alpha$, [N II] $\lambda$6583, [S II] $\lambda$6716, 6730, and [O III] $\lambda$5007 emission lines, and the Lick indices of the H$\beta$, Mgb, Fe5270, Fe5335 absorption lines (Worthey et al. 1994). The emission lines were analyzed by a Gaussian analysis of blends; in our Gaussian analysis of the H$\alpha$ + [N II] $\lambda$6548, 6583 blend we also took into account the H$\alpha$ absorption line of the stellar population. The line-of-sight velocities of the stellar component were determined by cross-correlating the spectra of the galaxy with the spectrum of the K3III giant star HD 10380 taken in the same spectrograph configuration. At distances from the center of more than $6''$ an additional binning of the spectra was used to increase the signal-to-noise ratio: in the ranges of distances from the center $6''$–$12''$, $12''$–$18''$, and $18''$–$28''$ we co-added, respectively, 11 (in 5.5-arcsec segments), 13 (in 6.5-arcsec segments), and 19 (in 9.5-arcsec segments) spectra; further out, we summed all spectra up to a distance of $38''$ from the center.

## RESULTS

### *The Rotation of Gas and Stars in IC 560*

Figure 1 presents the profiles of the measured line-of-sight velocities for the stars and ionized gas in IC 560. The rotation of stars can be traced to distances of about 30 arcsec from the center, or to 3.5 kpc. The ionized-gas velocities measured from several emission lines (H$\alpha$, [N II] $\lambda$6583, [S II] $\lambda$6717 + 6731, [O III] $\lambda$5007) are measurable only in the central part of the galaxy, $R<10''$, or to 1.1 kpc from the center. Note that the line-of-sight velocities measured from H$\alpha$ and from the forbidden nitrogen and oxygen lines slightly disagree; when a galaxy is observed nearly edge-on, this may suggest that a gas from regions with different kinematics and different type of excitation, for example, a gas excited by young stars in the disk and a gas excited at the edge of the bar by shock waves, falls on our line of sight. In the next section we will discuss the excitation of ionized gas at the center of IC 560 in more details, while here

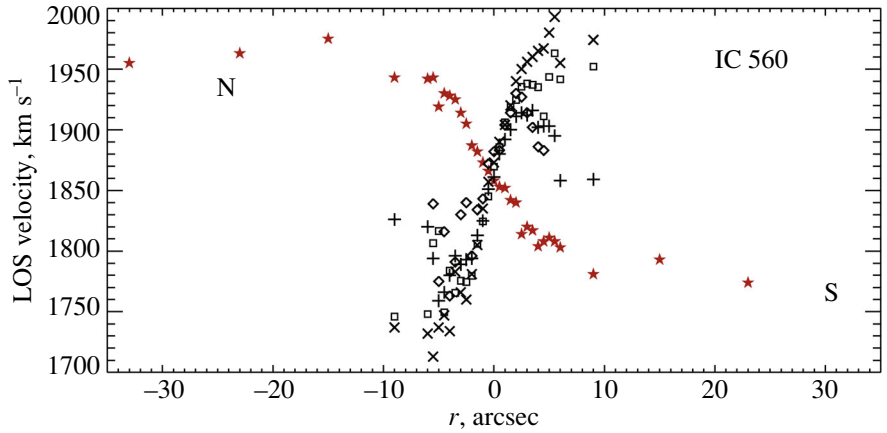


**Fig. 1.** Line-of-sight velocity distributions along the major axis of IC 560. The five-point stars mark the measurements for the stellar component; the remaining symbols correspond to the various ionized-gas emission lines: the crosses for H$\alpha$, the pluses for [N II] $\lambda$6583, the diamonds for [O III] $\lambda$5007, and the squares for [S II] $\lambda$6717 + 6731.

we can conclude that the ionized gas at the center of IC 560 rotates in a direction opposite to the direction of stellar rotation.

### *Characteristics of the Emission Gas in IC 560*

The spectrum of the central part of IC 560 rich in emission lines allowed some characteristics of the gas to be estimated from the intensity ratios of strong emission lines. First of all, we reached the conclusion about the source of gas ionization using the diagnostic BPT diagram. Baldwin et al. (1981) proposed to diagnose the pattern of gas excitation by comparing the intensity ratios of low- and high-excitation forbidden lines to the neighboring Balmer lines. The excitation of gas by photoionization (the blackbody spectra of O-type stars or an active nucleus with a power-law spectrum) and a shock wave can be distinguished on such BPT diagrams. We compared our measurements of the emission-line flux ratios in the range of distances from the center $4''-6''$, $\log([\mathrm{N\,II}]\ \lambda6583/\mathrm{H}\alpha) = -0.25 \pm 0.10$ and $\log([\mathrm{O\,III}]\ \lambda5007/\mathrm{H}\beta) = 0.20 \pm 0.15$ (in this case, the plus-minus is not the error of the mean but the dispersion of individual measurements) with the models from Kewley et al. (2006), with the measurements of the spectra for the nuclei of several thousand nearby galaxies from SDSS, and the models for the excitation of gas with different metallicities by shock waves from Allen et al. (2008) (Fig. 2). On the BPT diagram our measurements for the center of IC 560 are between the star-forming regions and shock waves. As we assumed in the previous section, this can be due to the simultaneous presence of ongoing star formation (young stars) and a bar producing shock fronts in the gas at its leading edge.

We can then estimate the gas electron density from the ratio of the sulfur doublet lines. In the range of distances from the center $4''-9''$ the mean [S II] $\lambda$6717/[S II] $\lambda$6731 ratio is $0.96 \pm 0.08$, and there is no gradient along the radius. A fairly high electron density, 350–500 cm$^{-3}$, according to the model calculations by Blair and Kirshner (1985), corresponds to this ratio of the sulfur doublet components. If it is compared with the typical data for circumnuclear star formation rings from Sarzi et al. (2007), then a comparable electron density in circumnuclear star formation regions is observed only in two galaxies, NGC 6951 and NGC 7217; all the remaining galaxies show a lower density.

Finally, we can estimate the gas metallicity by comparing the ratio of the nitrogen line to H$\alpha$ with that observed in H II regions with a well-measured emission spectrum. Using the calibration from Pettini and Pagel (2004), we find the oxygen abundance for the range of radii $4''-9''$ to be $12 + \log(\mathrm{O/H}) = 8.74 \pm 0.03$, i.e., slightly higher than the solar one if the young stars are assumed to dominate in the gas excitation. If, however, the shock waves are assumed to make a major contribution to the gas excitation, then, according to the calculations by Allen et al. (2008), the emission-line ratios in IC 560 in the range of radii $4''-6''$ are consistent with a gas metallicity from $-0.2$ to $+0.3$ dex, i.e., also near the solar value.

### *Star Formation Rates at the Center of IC 560*

References in the NED database show that the galaxy IC 560 was observed with the WISE infrared space telescope. This allows the star formation rate in the galaxy to be estimated from the mid-infrared flux. The galaxy turned out to be very bright at these wavelengths and was measured with a signal-to-noise ratio from $\sim$50 at 4 $\mu$m to 18 at 22 $\mu$m; we will use the measurements of the flux in the latter WISE

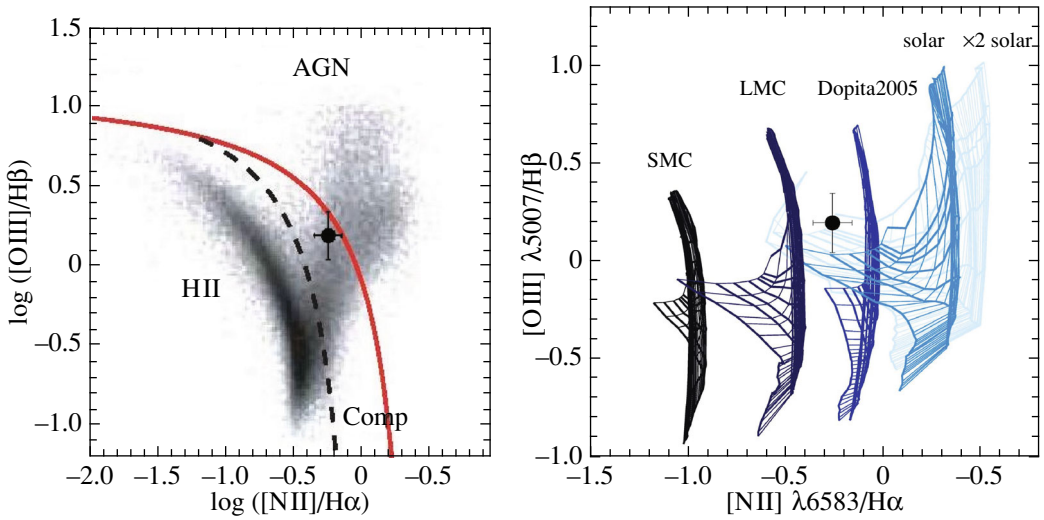


**Fig. 2.** Diagnostic diagrams to determine the gas excitation mechanism. According to Kewley et al. (2006), the emission-line intensity ratios for the gas excited by O stars and by active nuclei and shock waves are located, respectively, to the left of the dashed line and to the right of the solid line in Fig. 2a. The circle with error bars indicates our measurements for IC 560 in the range of radii 4″–6″; obviously, the gas with a high electron density is ionized by young stars, with the addition of shock waves. The models with gas excitation only by shock waves (Fig. 2b, Allen et al. 2008) are also consistent with our measured emission-line ratios if the gas metallicity is nearly solar (±0.3 dex).

photometric band related to hot dust to determine the star formation rate in IC 560. The spatial resolution of the WISE photometric observations varies from 6″ in the 3.4- and 4.6-$\mu$m bands to 12″ in the 22-$\mu$m band; when reducing the data for IC 560 in the latter band, the source was marked in the catalog as a point one, and, consequently, the magnitude determined by integration within the instrumental profile is an accurate integrated magnitude of the galaxy. We carried out a search at http://irsa.ipac.caltech.edu/cgi-bin/Radar/ in the WISE All-Sky Source Catalog subsection with a 10″ search cone and found only one point source for the center of IC 560, $W4mpro = 6.524 \pm 0.060$. From this magnitude, using the adopted distance to the galaxy of 23 Mpc and several calibrations of star formation rates from the literature (Rieke et al. 2009; Lee et al. 2013; Cluver et al. 2014), we estimated the star formation rate in the galaxy to be from 15 to 40 $M_\odot$ yr$^{-1}$!

The WISE multicolor photometric data also allow us to diagnose the excitation source, in this case, the source of dust heating, at the galactic center from a different perspective. The colors of the central 6 arcsec of IC 560, $[3.4] - [4.6] = -0.03$ and $[4.6] - [12] = 1.82$, place the galaxy in the region of normal *spiral* galaxies on the color–color diagram (Jarrett et al. 2011), i.e., they support the dust heating by young stars. According to Jarrett et al. (2011), the region of active galactic nuclei is bounded by the cutoffs $[3.4]-[4.6] > 0.5$ and $[4.6]-[12] > 2.2$. The high accuracy of the WISE measurements of IC 560, 0.02–0.03 mag in the 3.4-, 4.6-, and 12-$\mu$m bands, rules out the dust heating at the center of this galaxy by an active nucleus.

The NED database provides the integrated magnitudes of IC 560 in the $FUV$ and $NUV$ spectral bands measured with the GALEX space telescope: $m_{FUV} = 21.29$ and $FUV - NUV = 2.11$. We used the latter color index to find the slope of the spectrum in the ultraviolet using the formula from Overzier et al. (2011): $\beta_{\rm GALEX} = +2.69$. This slope suggests a huge amount of dust in IC 560, because the theoretical (unreddened) value of $\beta$ is $-2.23$ (Meurer et al. 1999). Using the calibration from Meurer et al. (1999), though outside the range of $\beta$ considered by them, we obtain a far-ultraviolet extinction estimate: $A_{1600} \approx 10$. Once we have corrected the integrated $FUV$ magnitude of IC 560 for this extinction, we estimate the integrated star formation rate from the $FUV$ flux using the calibrations from Lee et al. (2009): $SFR \approx 10\ M_\odot$ yr$^{-1}$. This is approximately consistent with the star formation rate estimated above from the flux at 22 $\mu$m.

### *Characteristics of Stellar Population in IC 560*

We detected an ionized gas with a solar chemical composition and ongoing star formation in the central kiloparsec of IC 560. Now we would like to understand the structural and evolutionary context in which this current star formation proceeds in a lenticular galaxy.

We analyzed the structure of the galaxy using a digital image of IC 560 from the public SDSS data archive. The results of our isophotal analysis of this

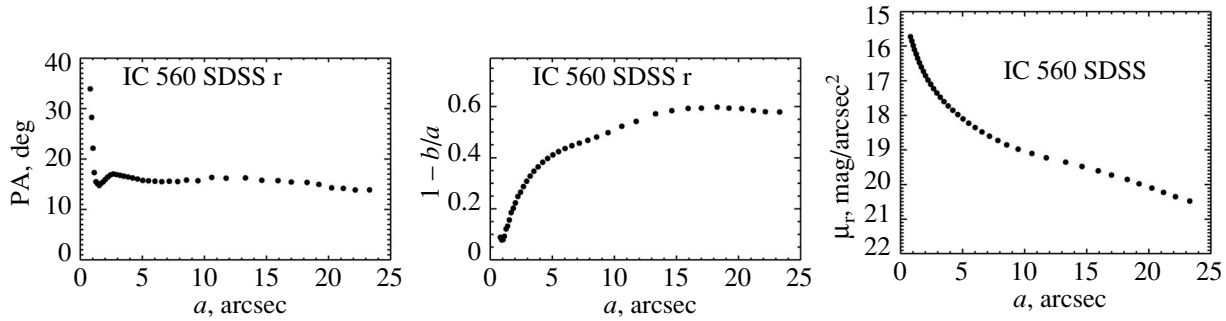


**Fig. 3.** Results of our isophotal analysis of the SDSS $r$-band image for IC 560. (a) the position angle of the major axis of the isophotes, (b) the ellipticity of the isophotes, and (c) the surface brightness profile averaged over the azimuth along the isophotes.

image are presented in Fig. 3. Since the galaxy is seen nearly edge-on, the monotonic and gradual increase in isophote ellipticity in the range of radii $1''-15''$ is obviously related to the presence of a fairly significant bulge. In the radial surface brightness profile this range of radii is characterized by a shape resembling the de Vaucouleurs law. Consequently, this confirms that the bulge dominates in the galaxy within $R < 15''$, and all of the star formation is concentrated inside the bulge. Accordingly, the large-scale stellar disk with an exponential surface brightness profile begins to dominate at radii $R > 15''$.

Let us now estimate the parameters of the stellar population by comparing the Lick indices with the evolutionary Simple Stellar Population (SSP) models computed for various magnesium-to-iron ratios by Thomas et al. (2003). It was necessary to correct the index of the H$\beta$ absorption line for the contribution from the emission component where it was present, i.e., within $R < 10''$. To calculate the correction, we used the equivalent width measurements for the H$\alpha$ emission line, which is always several times stronger than H$\beta$ in the ionized-gas spectrum. For the nucleus we applied a correction $\Delta = 0.25EW(\mathrm{H}\alpha)$ to the H$\beta$ index; for the remaining measurements referring to the regions of gas ionized by young stars we used the classical Balmer decrement $\mathrm{H}\alpha/\mathrm{H}\beta = 2.85$. Since this Balmer decrement disregards the presence of dust absorption, we definitely *overcorrect* the H$\beta$ index for the influence of emission, and the estimates of the mean age of the stellar population at the center of IC 560 presented below are actually a lower limit.

Figure 4 presents the diagnostic "index–index" diagrams where our measurements for IC 560 are compared with the models. The data points of our measurements are connected by a polygonal line in order of increasing radius to which the measurements refer. The big star is the nucleus, the next two points for $R = 5''$ and $9''$ refer to the region where a gas is present and star formation goes on, and the last two points, for $R = 15''$ and $23''$, refer to the outer disk where there are no gas and young stars. On the diagram comparing magnesium, Mgb, and iron, $\langle\mathrm{Fe}\rangle \equiv (\mathrm{Fe5270} + \mathrm{Fe5335})/2$, indices we see that at the center the ratio of the magnesium and iron abundances in stars is nearly solar, suggesting a long epoch of main star formation at the center of IC 560, while Mg/Fe in the disk increases sharply and approaches $[\mathrm{Mg/Fe}] = +0.3...+0.5$, which is equal to the elemental abundance ratio in Type II supernova ejecta and is typical of very short, $\Delta t < 1$ Gyr, star formation epochs. On the right two diagrams contrasting the H$\beta$ index with the composite metal-line index $[\mathrm{MgFe}] \equiv (\mathrm{Mgb}\langle\mathrm{Fe}\rangle)^{1/2}$, we can estimate the mean age and metallicity of the stellar population. In Fig. 4 we compare our measurements of H$\beta$ and $[\mathrm{MgFe}] \equiv (\mathrm{Mgb}\langle\mathrm{Fe}\rangle)^{1/2}$ with the models from Thomas et al. (2003) for $[\mathrm{Mg/Fe}]$ of 0.0 and +0.3. We see that when using the combined metal-line index, the age estimates depend weakly on the magnesium-to-iron ratio, but, nevertheless, it is better to use the diagram for $[\mathrm{Mg/\,Fe}] = 0.0$ for the central part of IC 560 and the diagram for $[\mathrm{Mg/Fe}] = +0.3$ for the disk. Since the models for low metallicities ($[\mathrm{Z/H}] < -0.4$) poorly compute the H$\beta$ index due to the uncertainties with the morphology of the horizontal branch and the lifetime of stars on it, we also plotted the observational data for several globular clusters in our Galaxy from Beasley et al. (2004) on these diagrams. According to the latest calibrations from Dias et al. (2016), three globular clusters in the bulge (NGC 6356, 6539, and 6838) have $[\mathrm{Fe/H}] = -0.6$, while the total metallicity, given their non-solar magnesium-to-iron ratio, is about $-0.4$. It can be seen from the diagrams in Fig. 4 that at an age of 10–12 Gyr they actually have an appreciably smaller H$\beta$ index than that predicted by the model. We see the same for the outer disk of IC 560: obviously, its stellar population has a metallicity $[\mathrm{Z/H}] \approx -1$ (see also the leftmost plot in Fig. 4) and an old age, $T > 10$ Gyr. The globular cluster NGC 6171, the fourth of those plotted

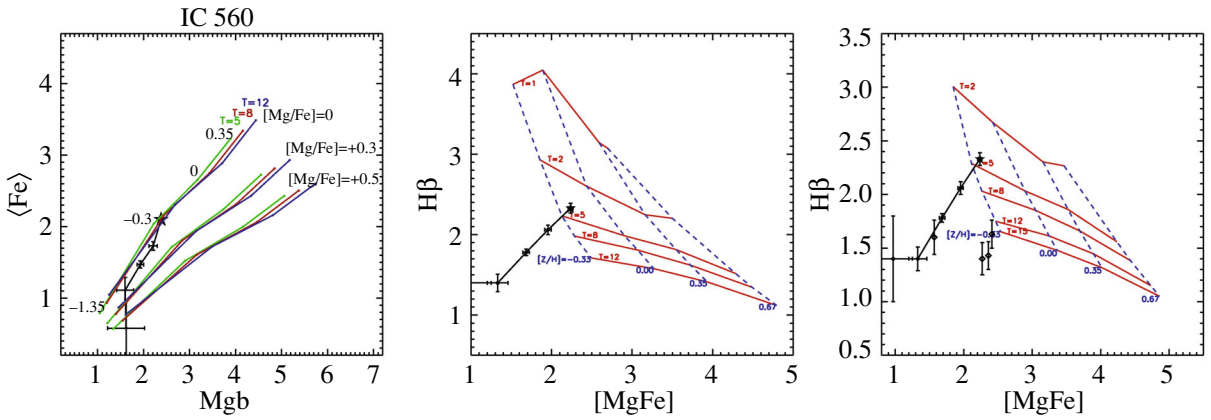


**Fig. 4.** Diagnostic "index–index" diagrams for the Lick indices in various stellar subsystems of IC 560 (filled circles with error bars). The small symbols connected by lines on the left panel and the solid lines on the two right panels represent the models of stellar populations with the same age (Thomas et al. 2003); the age of the models is in Gyr. The total metallicity of the models is indicated near the model reference points designated by small symbols on the left and connected by dashed lines on the right. On the diagnostic H$\beta$–[MgFe] diagrams we used the models with different magnesium-to-iron ratios: [Mg/Fe] = 0.0 at the center and [Mg/Fe] = +0.3 on the right.

in Fig. 4, falls exactly on the characteristics of the inner edge of the IC 560 disk; the metallicity of this globular cluster is [Fe/H] = −0.95 and [Mg/H] = −0.67 (Dias et al. 2016). The stellar nucleus of IC 560 has a mean age of ∼4 Gyr, which is consistent with an approximately constant star formation rate in the last 10 Gyr, and a metallicity [Z/H] = −0.3. The characteristics of the stellar population inside the galactic bulge are intermediate between the nucleus and the disk, but the metallicity of stars here is also too low for the center of a normal early-type galaxy, [Z/H] < −0.4.

## DISCUSSION

In the small lenticular galaxy IC 560 ($M_B$ = −18.3, HYPERLEDA) we detected a compact, ∼1 kpc in radius, circumnuclear disk of ionized gas with ongoing star formation; the star formation rate is roughly estimated to be 10–40 $M_\odot$ yr$^{-1}$. So far as is known, no molecular and neutral hydrogen is present in this galaxy (Young et al. 2011; Masters et al. 2014). The ionized gas disk rotates in the opposite direction to the rotation of the stellar component, of both the bulge and the disk. Despite the ongoing star formation, we found no evidence for the presence of a counter-rotating stellar component, possibly because the spectral resolution of our observations was not enough. The old stellar population of the outer galactic disk is very poor in metals ([Z/H] ≈ −1), which is an atypically low metallicity for a galaxy of such a luminosity. At the same time, the gas at the center exhibits a solar oxygen abundance. The mismatched kinematics of the gas and stars suggests an external origin of the gas, its accretion most likely from another galaxy, because accretion from a filament of the large-scale structure would give a low-metallicity gas. Thus, the problem of searching for the source of external gas accretion onto IC 560 becomes very acute, because we see nothing suitable for this role near the galaxy.

The galaxy IC 560 is officially a member of the NGC 2967 group (Garcia 1993; Giuricin et al. 2000), being ranked the second most massive one in this sparse group consisting exclusively of late-type galaxies (Makarov and Karachentsev 2011). It is almost 600 kpc away from to the group center, while the nearest neighbor, which is an order of magnitude less massive than IC 560, is only 115 kpc away. Thus, IC 560 is by no means an interacting galaxy and, in general, is located in a very rarefied environments. However, the fact that all members of the group are late-type galaxies with active star formation suggests that, in any case, the group has external (with respect to the galaxies) sources of cold gas that feed the star formation in all group members, including IC 560.

## ACKNOWLEDGMENTS

We thank the anonymous referee for drawing our attention to the infrared data of the WISE space telescope. All of the spectroscopic observations used in this study were obtained with the observing program 2012-2-RSA-OTH-002 at the Southern African Large telescope (SALT) supported by the National Research Foundation (NRF) of South Africa. When analyzing the data, we used the Lyon–Meudon Extragalactic Database (LEDA) maintained by the LEDA team at the CRAL Lyon Observatory and the NASA/IPAC Extragalactic Database (NED), which is operated by the Jet Propulsion Laboratory, the California Institute of Technology, under contract

with the National Aeronautics and Space Administration (USA). This study is partially based on the public data from the SDSS, SDSS-II, SDSS-III surveys (site http://www.sdss3.org/) financed by the Alfred P. Sloan foundation, the participating institutes of the SDSS collaboration, the National Science Foundation, the US Department of Energy, the National Aeronautics and Space Administration (USA), the Monbukagakusho Foundation (Japan), the Max Planck Society, and the Higher Education Funding Council for England. The study of the structure, dynamics, and evolution of disk galaxies was supported by the Russian Science Foundation (grant no. 14-22-00041).

## REFERENCES

1. M. G. Allen, B. A. Groves, M. A. Dopita, R. S. Sutherland, and L. J. Kewley, Astrophys. J. Suppl. **178**, 20 (2008).
2. J. A. Baldwin, M. M. Phillips, and R. Terlevich, Publ. Astron. Soc. Pacif. **93**, 5 (1981).
3. M. A. Beasley, J. P. Brodie, J. Strader, D. Forbes, R. N. Proctor, P. Barmby, and J. P. Huchra, Astron. J. **128**, 1623 (2004).
4. W. P. Blair and R. P. Kirshner, Astrophys. J. **289**, 582 (1985).
5. E. B. Burgh, K. H. Nordsieck, H. A. Kobulnicky, T. B. Williams, D. O'Donoghue, M. P. Smith, and J. W. Percival, Proc. Soc. Phot. Inst. Eng. **4841**, 1463 (2003).
6. M. Cappellari, E. Emsellem, D. Krajnovic, R. M. McDermid, N. Scott, G. A. Verdoes Kleijn, L. M. Young, K. Alatalo, et al., Mon. Not. R. Astron. Soc. **413**, 813 (2011).
7. M. E. Cluver, T. H. Jarrett, A. M. Hopkins, S. P. Driver, J. Liske, M. L. P. Gunawardhana, E. N. Taylor, A. S. G. Robotham, et al., Astrophys. J. **782**, 90 (2014).
8. S. M. Crawford, M. Still, P. Schellart, L. Balona, D. A. H. Buckley, G. Dugmore, A. A. S. Gulbis, A. Kniazev, M. Kotze, N. Loaring, K. H. Nordsieck, T. E. Pickering, S. Potter, E. Romero Colmenero, P. Vaisanen, T. Williams, and E. Zietsman, Proc. Soc. Phot. Inst. Eng. **7737**, 25 (2010).
9. T. A. Davis, K. Alatalo, M. Sarzi, M. Bureau, L. M. Young, L. Blitz, P. Serra, A. F. Crocker, et al., Mon. Not. R. Astron. Soc. **417**, 882 (2011).
10. B. Dias, B. Barbuy, I. Saviane, E. V. Held, G. S. da Costa, S. Ortolani, M. Gullieuszik, and S. Vasquez, Astron. Astrophys. **590**, Aid9 (2016).
11. E. Emsellem, M. Cappellari, D. Krajnović, K. Alatalo, L. Blitz, M. Bois, F. Bournaud, M. Bureau, et al., Mon. Not. R. Astron. Soc. **414**, 888 (2011).
12. A. M. Garcia, Astron. Astrophys. Suppl. Soc. **100**, 47 (1993).
13. G. Giuricin, C. Marinoni, L. Ceriani, and A. Pisani, Astrophys. J. **543**, 178 (2000).
14. T. H. Jarrett, M. Cohen, F. Masci, E. Wright, D. Stern, D. Benford, A. Blain, S. Carey, et al., Astrophys. J. **735**, 112 (2011).
15. I. Yu. Katkov, A. Yu. Kniazev, and O. K. Sil'chenko, Astron. J. **150**, 24 (2015).
16. L. J. Kewley, B. Groves, G. Kauffmann, and T. Heckman, Mon. Not. R. Astron. Soc. **372**, 961 (2006).
17. A. Y. Kniazev, A. A. Zijlstra, E. K. Grebel, L. S. Pilyugin, S. Pustilnik, P. Vaisanen, D. Buckley, Y. Hashimoto, N. Loaring, E. Romero, M. Still, E. B. Burgh, and K. Nordsieck, Mon. Not. R. Astron. Soc. **388**, 1667 (2008).
18. H. A. Kobulnicky, K. H. Nordsieck, E. B. Burgh, M. P. Smith, J. W. Percival, T. B. Williams, and D. O'Donoghue, Proc. Soc. Phot. Inst. Eng. **4841**, 1634 (2003).
19. K. Kuijken, D. Fisher, and M. R. Merrifield, Mon. Not. R. Astron. Soc. **283**, 543 (1996).
20. J. Ch. Lee, A. Gil de Paz, Ch. Tremonti, R. C. Kennicutt, Jr., S. Salim, M. Bothwell, D. Calzetti, J. Dalcanton, et al., Astrophys. J. **706**, 599 (2009).
21. J. Ch. Lee, H. S. Hwang, and J. Ko, Astrophys. J. **774**, id. 62 (2013).
22. D. Makarov and I. Karachentsev, Mon. Not. R. Astron. Soc. **412**, 2498 (2011).
23. K. L. Masters, A. Crook, T. Hong, T. H. Jarrett, B. S. Koribalski, L. Macri, Ch. M. Springob, and L. Staveley-Smith, Mon. Not. R. Astron. Soc. **443**, 1044 (2014).
24. G. R. Meurer, T. M. Heckman, and D. Calzetti, Astrophys. J. **521**, 64 (1999).
25. R. A. Overzier, T. M. Heckman, J. Wang, L. Armus, V. Buat, J. Howell, G. Meurer, M. Seibert, et al., Astrophys. J. Lett. **726**, L7 (2011).
26. M. Pettini and B. E. J. Pagel, Mon. Not. R. Astron. Soc. **348**, L59 (2004).
27. G. H. Rieke, A. Alonso-Herrero, B. J. Weiner, P. G. Pérez-González, M. Blaylock, J. L. Donley, and D. Marcillac, Astrophys. J. **692**, 556 (2009).
28. L. J. Sage and G. A. Welch, Astrophys. J. **644**, 850 (2006).
29. M. Sarzi, E. L. Allard, J. H. Knapen, and L. M. Mazzuca, Mon. Not. R. Astron. Soc. **380**, 949 (2007).
30. D. Thomas, C. Maraston, and R. Bender, Mon. Not. R. Astron. Soc. **339**, 897 (2003).
31. G. A. Welch and L. J. Sage, Astrophys. J. **584**, 260 (2003).
32. G. Worthey, S. M. Faber, J. J. Gonzalez, and D. Burstein, Astrophys. J. Suppl. Ser. **94**, 687 (1994).
33. L. M. Young, M. Bureau, T. A. Davis, F. Combes, R. M. McDermid, K. Alatalo, L. Blitz, M. Bois, et al., Mon. Not. R. Astron. Soc. **414**, 940 (2011).

*Translated by N. Samus'*